



University of Groningen

Effects of rhamnolipid biosurfactants on removal of phenanthrene from soil

Noordman, Wouter H.; Ji, Wei; Brusseau, Mark L.; Janssen, Dick B.

Published in:
Environmental science & technology

DOI:
[10.1021/es970739h](https://doi.org/10.1021/es970739h)

IMPORTANT NOTE: You are advised to consult the publisher's version (publisher's PDF) if you wish to cite from it. Please check the document version below.

Document Version
Publisher's PDF, also known as Version of record

Publication date:
1998

[Link to publication in University of Groningen/UMCG research database](#)

Citation for published version (APA):

Noordman, W. H., Ji, W., Brusseau, M. L., & Janssen, D. B. (1998). Effects of rhamnolipid biosurfactants on removal of phenanthrene from soil. *Environmental science & technology*, 32(12), 1806-1812.
<https://doi.org/10.1021/es970739h>

Copyright

Other than for strictly personal use, it is not permitted to download or to forward/distribute the text or part of it without the consent of the author(s) and/or copyright holder(s), unless the work is under an open content license (like Creative Commons).

Take-down policy

If you believe that this document breaches copyright please contact us providing details, and we will remove access to the work immediately and investigate your claim.

Downloaded from the University of Groningen/UMCG research database (Pure): <http://www.rug.nl/research/portal>. For technical reasons the number of authors shown on this cover page is limited to 10 maximum.

Effects of Rhamnolipid Biosurfactants on Removal of Phenanthrene from Soil

WOUTER H. NOORDMAN,[†] WEI JI,[‡]
MARK L. BRUSSEAU,^{‡,§} AND
DICK B. JANSSEN^{*†}

Department of Biochemistry, Groningen Biomolecular Sciences and Biotechnology Institute, University of Groningen, Nijenborgh 4, 9747 AG Groningen, The Netherlands, Soil, Water and Environmental Science Department, and Hydrology and Water Resources Department, University of Arizona, Tucson, Arizona 85721

Solubilizing agents may enhance remediation of soils contaminated with hydrophobic organic contaminants by diminishing sorption of the contaminants or increasing desorption rates. The effectiveness of rhamnolipid biosurfactants to enhance the removal of sorbed contaminants from soil was determined using column studies. Soil columns were contaminated with phenanthrene and subsequently eluted with electrolyte solution or with electrolyte solution containing 500 mg/L rhamnolipid. For the four soils studied, removal of 50% of the phenanthrene from the soil columns was accomplished in a 2–5-fold shorter time period, and the time required for 90% removal was reduced up to 3.5-fold when elution was performed with the rhamnolipid-containing solution as compared to the treatment without rhamnolipid. The effect of rhamnolipid on the removal of phenanthrene was satisfactorily simulated using independently obtained parameters with a two-component advective–dispersive model accounting for micellar solubilization and admicellar sorption. A more detailed analysis of the system showed that desorption rates of phenanthrene in the presence of 500 mg/L rhamnolipid were higher than predicted on the basis of desorption rate constants of phenanthrene determined in the absence of rhamnolipid. It is concluded that rhamnolipid enhanced the removal of phenanthrene mainly by micellar solubilization and also by influencing sorption kinetics.

Introduction

To enhance remediation of soils contaminated with hydrophobic organic contaminants (HOC), agents might be used in aquifer remediation that diminish sorption of HOC and increase desorption rates. Compounds tested in laboratory experiments include dissolved organic matter (1–3), cyclodextrin (4), organic cosolvents (5–7), and surfactants (8–12). It has been established that these agents can enhance the removal of HOC by influencing sorption equilibria. Much

less is known about the effects of these agents on desorption kinetics.

Biosurfactants have advantages as compared to synthetic compounds for use in soil remediation as biosurfactants are natural compounds that will have a low environmental impact. Thus, complete removal after treatment may not be necessary. In situ production may also be possible. To be effective for enhancing the removal of sorbed contaminants, a biosurfactant should have high solubilizing properties, should be water soluble, and should not strongly adsorb to soil. On the basis of these criteria, a rhamnolipid biosurfactant was selected for our studies. Rhamnolipid is a mixture of α -L-rhamnopyranosyl- β -hydroxyalkanoyl- β -hydroxyalkanoates and 2-O- α -L-rhamnopyranosyl- α -L-rhamnopyranosyl- β -hydroxyalkanoyl- β -hydroxyalkanoates. These anionic glycolipids are produced by various *Pseudomonas* species. It has been shown that this biosurfactant can stimulate the degradation of several organic compounds (13–15), influence the sorption of HOC to soil (16), and increase the solubility of heavy metals (17). The goal of this work was to determine whether rhamnolipid biosurfactants can enhance the removal of sorbed hydrophobic contaminants from soil and to obtain insight in the processes involved. Phenanthrene, a three-ring polycyclic aromatic hydrocarbon, was used as a model compound.

Model Development

Sorption of Phenanthrene. Sorption of phenanthrene was described using a model that conceptualizes soil as consisting of a domain for which sorption is instantaneous (domain 1, fraction F) and a domain for which sorption is rate-limited (domain 2, fraction $1 - F$) (18). A first-order equation was used to describe mass transfer between the two sorptive domains:

$$\text{HOC(aq)} \xrightleftharpoons[k_{-1}k_{-1'}]{FK_d} \text{HOC(domain 1)} \xrightleftharpoons[k_{-1}k_{-1'}]{k_1k_1'} \text{HOC(domain 2)}$$

$$S_{\text{HOC},1} = FK_d C_{\text{HOC,aq}} \quad (1)$$

$$\frac{\delta S_{\text{HOC},2}}{\delta t} = k_{-1}((1-F)K_d C_{\text{HOC,aq}} - S_{\text{HOC},2}) \quad (2)$$

where $C_{\text{HOC,aq}}$ is the dissolved aqueous HOC concentration (g/L); $S_{\text{HOC},1}$ and $S_{\text{HOC},2}$ are the concentrations of sorbed phenanthrene in the instantaneous and rate-limited domains, respectively (g/kg); K_d is the sorptive partitioning constant of phenanthrene (L/kg); k_1 and k_{-1} are first-order rate constants (h^{-1}), associated with the sorption and desorption processes, respectively; k_1' and k_{-1}' are the respective rate constants in the presence of surfactant (h^{-1}).

Micelle Partitioning. Above a critical micelle concentration (cmc), surfactants form micellar aggregates into which hydrophobic compounds partition (19). When the surfactant concentration was higher than the cmc, partitioning of HOC into micelles was described using:

$$C_{\text{HOC,mic}} = K_c(C_{\text{surf}} - \text{cmc})C_{\text{HOC,aq}} \quad (3)$$

where $C_{\text{HOC,mic}}$ is the concentration of micelle-partitioned HOC (g/L), K_c is a mass-based micelle partitioning constant (L/g) (3, 4), and C_{surf} is the aqueous surfactant concentration (g/L). Micellar partitioning reduces sorption of HOC to soil through reducing $C_{\text{HOC,aq}}$ (eqs 1–3). Partitioning of com-

* Corresponding author e-mail: D.B.Janssen@chem.rug.nl; telephone: +31-50 363 4209; fax: +31-50 363 4165.

[†] Department of Biochemistry.

[‡] Soil, Water and Environmental Science Department.

[§] Hydrology and Water Resources Department.

pounds from the water phase into surfactant micelles is generally considered an extremely fast process (20, 21).

Sorption of Rhamnolipid. Adsorption of rhamnolipid to soil was described using the Langmuir isotherm (22). Flow interruption experiments (23) have shown that adsorption of rhamnolipid to soil was fast on the time scale of our column experiments (data not shown).

Admicellar Sorption. Adsorbed surfactant, referred to as admicelles, provides additional sorptive capacity to the soil, which enhances sorption of HOC (24–26). Admicellar sorption was described using an admicellar partitioning constant K_{admic} (L/g) (25, 27–29):

$$S_{\text{HOC,admic}} = K_{\text{admic}} S_{\text{surf}} C_{\text{HOC,aq}} \quad (4)$$

where $S_{\text{HOC,admic}}$ is the concentration of phenanthrene partitioned into admicelles (g/kg) and S_{surf} is the concentration of adsorbed surfactant (g/kg). K_{admic} was assumed to be equal to K_c as micelles and admicelles are similar structures. Though the general validity of this assumption is not established, it is supported by empirical results from various systems (25–27). Admicellar sorption is considered to be instantaneous, since transfer of aqueous HOC to the vicinity of the admicelle and incorporation of HOC into the admicelle (similar to partitioning into micelles) are both assumed to be rapid relative to the time scale of our experiments.

Transport. The equations presented above were incorporated into a two-component advective–dispersive equation to yield a model describing the simultaneous transport of a contaminant and a solubilizing agent. Transport of the solubilizing agent is assumed to be independent of HOC and is described with a traditional advective–dispersive equation using a Langmuir isotherm under equilibrium conditions to account for adsorption of the agent (22). Accounting for all the processes as described above, the advective–dispersive equation for the contaminant is

$$\begin{aligned} \frac{\partial C_{\text{HOC,aq}}}{\partial t} + \frac{\partial C_{\text{HOC,mic}}}{\partial t} + \frac{\rho}{\theta} \frac{\partial S_{\text{HOC,1}}}{\partial t} + \frac{\rho}{\theta} \frac{\partial S_{\text{HOC,2}}}{\partial t} + \\ \frac{\rho}{\theta} \frac{\partial S_{\text{HOC,admic}}}{\partial t} = D \frac{\partial^2 C_{\text{HOC,aq}}}{\partial x^2} + D \frac{\partial^2 C_{\text{HOC,mic}}}{\partial x^2} - v \frac{\partial C_{\text{HOC,aq}}}{\partial x} - \\ v \frac{\partial C_{\text{HOC,mic}}}{\partial x} \quad (5) \end{aligned}$$

where ρ is the bulk density of the soil (kg/L), θ is the porosity of the soil (L/L), v is the pore water velocity (cm/h), and D is the dispersion coefficient (cm²/h). Equations 1–5 can be converted to the following dimensionless equations:

$$\begin{aligned} \beta' R \frac{\partial C_{\text{HOC}}^*}{\partial T} + E(1 - \beta') R \frac{\partial S_{\text{HOC,2}}^*}{\partial T} + C_{\text{HOC}}^* \frac{\partial (\beta' R)}{\partial T} = \\ \frac{1}{Pe} \frac{\partial^2 C_{\text{HOC}}^*}{\partial X^2} - \frac{\partial C_{\text{HOC}}^*}{\partial X} \quad (6) \end{aligned}$$

$$(1 - \beta') R \frac{\partial S_{\text{HOC,2}}^*}{\partial T} = \omega' \left(\frac{C_{\text{HOC}}^*}{E} - S_{\text{HOC}}^* \right) \quad (7)$$

with

$$E = 1 + K_c (C_{\text{surf}} - \text{cmc}) \quad (8)$$

$$R' = 1 + \frac{\rho}{\theta} \frac{K_d}{E} + \frac{\rho}{\theta} \frac{K_{\text{admic}} S_{\text{surf}}}{E} \quad (9)$$

$$\beta' = \left[1 + \frac{\rho}{\theta} \frac{FK_d}{E} + \frac{\rho}{\theta} \frac{K_{\text{admic}} S_{\text{surf}}}{E} \right] / R' \quad (10)$$

$$\omega' = k_{-1}' (1 - \beta') R' L / v \quad (11)$$

$$\begin{aligned} C_{\text{HOC}}^* &= (C_{\text{HOC,aq}} + C_{\text{HOC,mic}}) / C_{\text{HOC,0}} \\ S_{\text{HOC,2}}^* &= S_{\text{HOC,2}} / ((1 - F) K_d C_{\text{HOC,0}}) \end{aligned}$$

$$Pe = vL/D \quad X = x/L \quad T = vt/L$$

where C_{HOC}^* is the dimensionless concentration of HOC in the aqueous phase (dissolved plus micellar solubilized), $S_{\text{HOC,2}}^*$ is the dimensionless concentration of HOC in the rate-limited domain, $C_{\text{HOC,0}}$ is the aqueous HOC concentration in the influent during contamination of the column (g/L), L is the column length (cm), and Pe is the Peclet number. R' , β' and ω' are the retardation factor, the fraction of instantaneous retardation, and the Damkohler number of HOC in the presence of surfactant, respectively. E is the enhancement factor, which represents the reduction of sorption due to micellar partitioning. E , R' , β' , ω' , and k_{-1}' are functions of the surfactant concentration and thus change in place and time. Equations 5 and 6 were solved using the Crank–Nicolson method. A flux-type boundary condition was used at the inlet, and a Neumann-type boundary condition was used at the outlet. The initial condition with $C_{\text{HOC}}(x,0) = C_{\text{surf}}(x,0) = 10^{-10}$ g/L was used to approximate an uncontaminated column. It is assumed that dispersion of the conservative tracer, phenanthrene, and rhamnolipid can be described using the same Peclet number (i.e., mechanical mixing controls dispersion) (30, 31).

When the concentration of surfactant is constant or when surfactant is absent, the functions R' , β' , and ω' become constants. In these cases, the last term on the left-hand side of eq 6 drops out to yield an equation that contains the same terms as the traditional transport equation but uses the constants R' , β' , and ω' . In the absence of surfactant, R' , β' , and ω' (eqs 9–11) reduce to

$$R = 1 + \frac{\rho}{\theta} K_d \quad (12)$$

$$\beta = \left(1 + \frac{\rho}{\theta} FK_d \right) / R \quad (13)$$

$$\omega = k_{-1} (1 - \beta) RL / v \quad (14)$$

where R is the retardation factor, β is fraction of instantaneous retardation, and ω is the Damkohler number in the absence of surfactant.

Materials and Methods

Chemicals, Soils, and Solutions. Phenanthrene (99+% purity) and pentafluorobenzoic acid (PFBA, 99%) were obtained from Acros (Geel, Belgium). Soils were air-dried and sieved (<2 mm) prior to use. In all experiments, a background electrolyte solution was used that contained 10 mM KNO₃, 3 mM NaN₃ (to suppress microbial activity), and 10 mM Tris-HCl, pH 7.0, in Milli-Q water. The buffer was used to maintain a constant pH, given that rhamnolipid behavior is strongly pH dependent (13, 32, 33).

Rhamnolipid. Rhamnolipid was produced by *Pseudomonas aeruginosa* UG2 (16), isolated from the culture fluid by a series of consecutive steps of acid precipitation and dissolution in 50 mM NaHCO₃ (13), and purified by column chromatography over Sephadex LH20 with methanol as the eluent. The purified rhamnolipid was dissolved in 10 mM NaHCO₃ to a concentration of about 40 mg/mL. The rhamnolipid concentration in this stock solution was determined using the 6-deoxyhexose assay with L-rhamnose as a standard (34), an average molecular weight of 588, and a rhamnose content (w/w) of 0.44.

TABLE 1. Physical Properties of Soils Used

	sand (%)	silt (%)	clay (%)	organic C (%)	ρ (kg/L)	θ (-)	literature
Eustis	95.1	2.2	2.7	0.27	1.54	0.36	18, 46
Borden	>99	<1	<1	0.03	1.58	0.38	18, 36
Vinton	94.5	2.8	2.7	0.09	1.53	0.35	47
Bonify	91.2	3.3	5.5	0.36	1.77	0.33	

Determination of cmc and Micelle Partitioning Constant. The cmc of rhamnolipid in electrolyte solution was determined to be 20 mg/L from the onset of the increase in solubility of phenanthrene. The micelle partitioning constant was determined from the increase in apparent solubility of phenanthrene (dissolved plus micelle partitioned) with increasing concentration of rhamnolipid (19). Solutions containing 0–700 mg/L rhamnolipid were saturated with phenanthrene by repeated application to a column packed with phenanthrene-coated Chromosorb GAW (Chrompack, Bergen op Zoom, The Netherlands) (35).

Column Experiments. All (sub)soils except Bonify soil were packed in 7 cm long, 2.25 cm i.d. stainless steel preparative HPLC columns provided with distributor disks and stainless steel frits (0.5 μ m pore diameter, Alltech Associated Inc.). Bonify soil was packed into a 5 cm long, 2.6 cm i.d. plexiglass column because this soil caused high-pressure buildup in columns with stainless steel frits. All soils were dry packed in incremental steps. Solutions were delivered to the column using a HPLC single-piston pump (Scientific Systems Inc., State College, PA). Stainless steel tubing (0.8 mm i.d.) was used for all connections. Independent experiments in the absence of a soil matrix confirmed that sorption of phenanthrene to the apparatus was minimal.

After packing, columns were slowly wetted with electrolyte solution until saturation was complete. The first few milliliters of solution were pale brown, indicating minor leaching of organic matter. More than 100 pore volumes of electrolyte solution were passed through the column to condition the matrix. The bulk density and porosity were determined gravimetrically (Table 1). Flow rates in subsequent experiments were 0.4 mL/min (20 cm/h) for Borden, 0.6 mL/min (26 cm/h) for Vinton, and 2 mL/min (90 cm/h) for Eustis and Bonify soils. Flow rates were measured gravimetrically and were found to be constant within 2% during the course of experiments. Effluent was directed to a fraction collector with 14 mm wide, 150 mm long tubes and analyzed for rhamnolipid and phenanthrene within 14 h. Total recovery of phenanthrene and rhamnolipid varied from 96% to 102% and from 99% to 116%, respectively. During all experiments, the pH remained constant at 7.0–7.1 except for Borden material. In this material, the pH remained at 7.7, presumably due to the high carbonate content of this soil (36). PFBA breakthrough curves were sigmoidal in shape and showed no tailing, indicating that physical nonequilibrium effects were absent and that columns were packed homogeneously. Peclet numbers were found to be higher than 120, except for the Bonify column where the Peclet number was 20.

Rhamnolipid-Enhanced Removal and Transport. The impact of rhamnolipid on phenanthrene removal was studied by introducing a phenanthrene-containing solution (1 mg/L) into the soil-packed columns. Subsequently, the columns were eluted either with electrolyte solution or with electrolyte solution containing rhamnolipid (500 mg/L). After removal of phenanthrene, rhamnolipid was removed from the column by elution with electrolyte solution to determine the recovery of rhamnolipid. The transport of phenanthrene in the presence of a background concentration of rhamnolipid was

examined by introducing a solution containing phenanthrene (1 mg/L) and rhamnolipid (20 or 500 mg/L) into a column that was pre-equilibrated with the same concentration of rhamnolipid. After breakthrough of phenanthrene was complete, the phenanthrene was eluted from the column using the rhamnolipid-containing solution.

Analytical Procedures. Column effluent was analyzed for PFBA using a flow-through variable wavelength detector at 250 nm. Aqueous rhamnolipid concentrations were determined with surface tension measurements using a Fischer model 21 du Nouy ring tensiometer (Pittsburgh, PA). Aqueous phenanthrene concentrations (dissolved plus micelle partitioned) were determined with fluorescence spectroscopy using a Hitachi F-200 fluorescence spectrophotometer (Hitachi, Ltd., Tokyo, Japan). The excitation and emission wavelengths were 246 and 366 nm, respectively. Solutions were diluted 10–100-fold to concentrations where the fluorescence signal was linear with the phenanthrene concentration and independent of the concentration of rhamnolipid present. Phenanthrene concentrations (dissolved plus micelle partitioned) for the experiment presented in Figure 5 were determined by HPLC using a Merck L-6200 pump (Hitachi, Ltd.), a Chromosphere PAH 100 mm column (Chrompack), a Merck L-4200 UV-vis detector (Hitachi, Ltd.), and an 150 μ L injection loop. The mobile phase consisted of 55% acetonitrile and 45% water. The experimental error was 3%, both for the fluorescence and the HPLC method.

Quantitative Analysis. Breakthrough curves of the conservative tracer PFBA were analyzed with a local equilibrium advective–dispersive transport model to determine the Peclet number using the computer program CXTFIT (37). The retardation factor for rhamnolipid (R_{RL}) was determined from the area above the frontal limb of the rhamnolipid breakthrough curve. The Langmuir isotherm coefficients $S_{max,RL}$ (mg/kg) and K_{RL} (L/mg) were chosen such as to describe the frontal and distal portions of the rhamnolipid breakthrough curve with the constraint that $1 + \rho/\theta(S_{max,RL}K_{RL}/(K_{RL}C_0 + 1)) = R_{RL}$. The retardation factor for phenanthrene in the absence of rhamnolipid was determined from moment analysis (38). The parameters β and ω were subsequently determined by optimization using an advective–dispersive transport model based on the two-domain sorption conceptualization (eqs 1–2) with the program CXTFIT. From these parameters, K_d , F , and k_{-1} were calculated according to eqs 12–14.

Rhamnolipid-enhanced removal curves were simulated using the model described by eqs 6–11 using independently obtained parameters. It was assumed that rhamnolipid did not influence the first-order desorption rate constant of phenanthrene (i.e., $k_{-1}' = k_{-1}$), unless explicitly mentioned otherwise. Both the frontal and distal portion of the elution profile were simulated in one run to account for a possibly nonhomogeneous distribution of phenanthrene in the column at the start of elution with rhamnolipid. The potential impact of a difference in the mobility of the various rhamnolipid species on removal of phenanthrene was neglected because the retardation of rhamnolipid was much smaller than that of phenanthrene, and any effect would be limited to a small number of pore volumes. Phenanthrene breakthrough curves in the presence of a constant rhamnolipid background concentration were calculated with CXTFIT using the parameters R' as determined by moment analysis, β' as calculated from eq 10 (assuming F is unchanged in the presence of rhamnolipid), and ω' as calculated from eq 11 using $k_{-1}' = k_{-1}$; $k_{-1}' = 3k_{-1}$; or $k_{-1}' \rightarrow \infty$.

The number of pore volumes required to remove 50% or 90% of the phenanthrene initially present in the columns was determined by comparing the area above the frontal limb and the area below the distal limb of the phenanthrene elution curves.

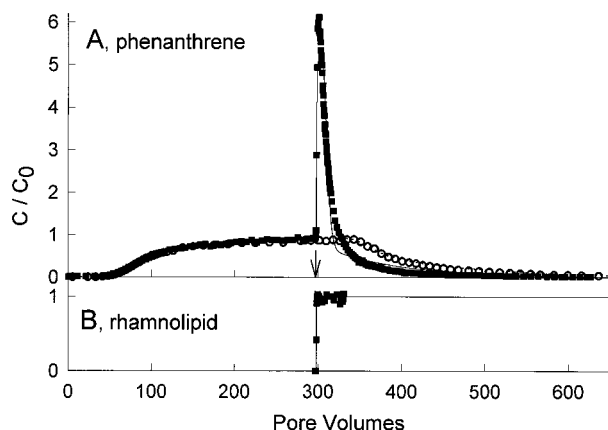


FIGURE 1. Rhamnolipid-enhanced removal of phenanthrene from Eustis soil. Columns were eluted with a solution containing phenanthrene ($C_{phen,0}$). At the time indicated by the arrow, the column was eluted with a phenanthrene-free solution either containing no rhamnolipid or containing 500 mg/L rhamnolipid ($C_{RL,0}$). (A) Breakthrough curve of phenanthrene when elution was performed without rhamnolipid (\circ , dotted line shows best fit) or with rhamnolipid (\blacksquare , solid line shows simulated). (B) Experimental (\blacksquare) and simulated (—) breakthrough curve of rhamnolipid during phenanthrene removal.

Results and Discussion

The equilibrium constant for partitioning of phenanthrene between solution and rhamnolipid micelles, K_c , was determined as 9.38 L/g ($n = 10$, $r^2 = 0.99$), or a log K_m (mole-fraction-based micelle partitioning constant (19)) of 5.50. This value is equivalent to a previously reported value (39). No enhanced solubility of phenanthrene was detected at rhamnolipid concentrations below the cmc.

To examine the impact of rhamnolipid on phenanthrene removal, soils were first contaminated by introducing a phenanthrene-containing solution into the columns (Figures 1 and 2). The transport of phenanthrene in all four soils was characterized by early breakthrough and extended tailing, showing that transport of phenanthrene was strongly influenced by nonequilibrium effects. The breakthrough curves were generally described well by the two-domain model as given by eqs 1–2 ($r^2 \geq 0.99$, Table 2, Figures 1 and 2). Duplicate experiments showed less than 10% variation in K_d and less than 25% in k_{-1} . With an increase in soil organic carbon content (Table 1), K_d increased and k_{-1} decreased (Table 2), as expected (40). As the two-domain model is a simplification of the real system, k_{-1} should be seen as a mass transfer coefficient that together with F best characterizes the rate-limited sorption observed under the experimental conditions. Average phenanthrene loadings in the columns at the start of elution were 33, 2, 4, and 26 mg/kg in Eustis, Borden, Vinton, and Bonify soils, respectively.

Rhamnolipid-Enhanced Removal of Phenanthrene.

After contamination, the soil columns were eluted either with electrolyte solution or with electrolyte solution containing 500 mg/L rhamnolipid (Figures 1 and 2). The phenanthrene elution curves in the absence of rhamnolipid were the reverse of the frontal limb of the breakthrough curve, as predicted for compounds with linear, reversible sorption. When the contaminated soils were eluted with a solution containing rhamnolipid, biosurfactant effluent concentrations reached influent concentrations after several pore volumes (Figure 1B). The retardation factors for rhamnolipid in Eustis, Borden, Vinton, and Bonify soils were 1.2, 2.0, 1.9, and 1.3, respectively. The fast and complete breakthrough of rhamnolipid was described satisfactorily using the Langmuir isotherm (e.g., Figure 1B) using the parameters $S_{max,RL} = 24$, 290, 100, and 28 mg/kg and $K_{RL} = 0.20$, 0.0013, 0.20, and 0.20

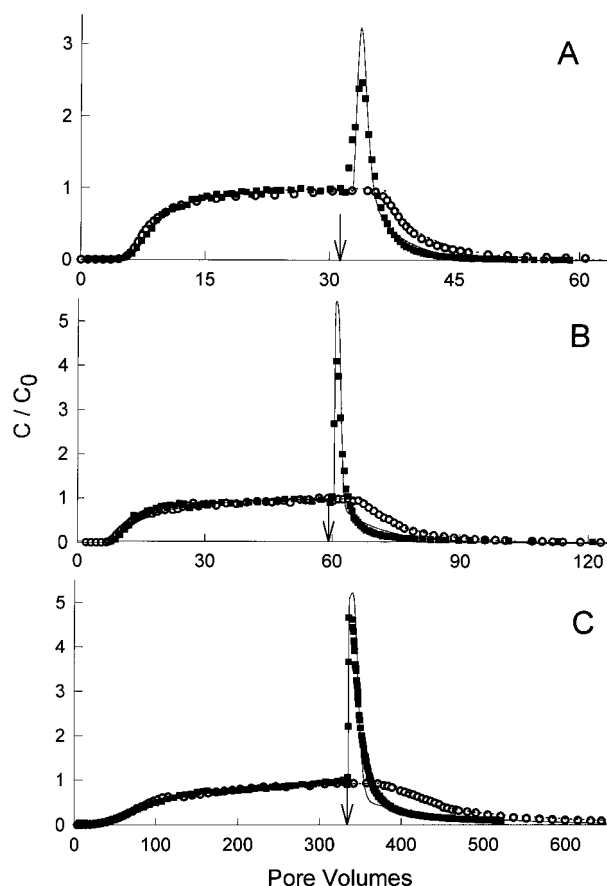


FIGURE 2. Rhamnolipid-enhanced removal of phenanthrene from (A) Borden material, (B) Vinton soil, and (C) Bonify soil. Details as described in Figure 1.

L/mg for Eustis, Borden, Vinton, and Bonify soils, respectively. Concurrent with breakthrough of rhamnolipid, the effluent phenanthrene concentration increased to values higher than the concentration with which the columns had been contaminated ($C_{HOC,0}$). As phenanthrene partitioned into rhamnolipid micelles, sorption of phenanthrene to soil decreased, and excess phenanthrene was removed.

Simulation of Phenanthrene Removal. The height and shape of the peak in phenanthrene effluent concentration on breakthrough of rhamnolipid as well as the prolonged tailing of phenanthrene were simulated well by the two-component model (eqs 6–11) using independently obtained parameters (Figures 1 and 2). These results suggest that the description of the enhanced removal process with solubilization and admicellar sorption provides an accurate representation of this system. The model simulations were not sensitive to the precise values of $S_{max,RL}$ and K_{RL} as the shape of the breakthrough front of the solubilizing agent was insensitive of these parameters as long as $K_{RL}C_{RL,0} > 1$. Because the adsorption of rhamnolipid to all soils studied was low relative to sorption of phenanthrene, the contribution of admicellar sorption of phenanthrene to the overall process was negligible, and simulations were not sensitive to the value of K_{admic} . Therefore, the assumption that $K_{admic} = K_c$ could not be verified.

The effluent phenanthrene concentration is expected to increase by the factor E (5.7 at 500 mg/L rhamnolipid) at breakthrough of rhamnolipid when enough phenanthrene is present in the equilibrium domain to establish the new equilibrium. This was indeed observed for Eustis and Bonify soils (Figures 1 and 2C). For the soils with lower sorption

TABLE 2. Phenanthrene Transport Parameters Determined from Breakthrough Curves

soil	[RL] ^a = 0 mg/L					[RL] ^a = 500 mg/L		[RL] ^a = 20 mg/L	
	<i>R</i>	<i>K_d</i> (L/kg)	<i>F</i> ^b (—)	<i>k₋₁</i> ^b (h ⁻¹)	<i>r</i> ² ^c	<i>R</i> '	<i>R</i> ' _{predicted} ^d	<i>R</i> '	<i>R</i> ' _{predicted} ^d
Eustis	141	33	0.52 ± 0.01	0.15 ± 0.01	0.990	31	26	129	142
		30 ^e	0.43 ± 0.01	0.19 ± 0.01	0.99				
Borden	10.5	2.3	0.60 ± 0.01	0.61 ± 0.05	0.993	7.2	3.5		
		2.2 ^e	0.66 ± 0.01	0.51 ± 0.05	0.99				
Vinton	18	3.9	0.53 ± 0.01	0.45 ± 0.02	0.994				
Bonify	143	26	0.52 ± 0.01	0.14 ± 0.01	0.994				

^a Concentration of rhamnolipid in background solution. ^b Optimized value ± one standard deviation. ^c Goodness of fit, from CXTFIT. ^d Predicted retardation factor for phenanthrene in the presence of rhamnolipid, calculated according to eq 11. ^e Duplicate experiment.

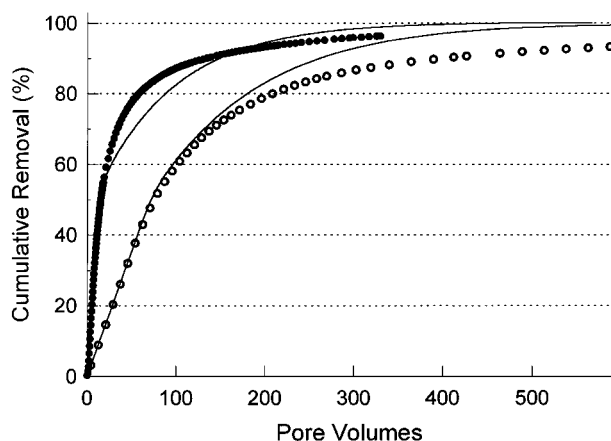


FIGURE 3. Cumulative removal of phenanthrene from Eustis soil when elution was performed without rhamnolipid (○, dotted line shows best fit) or with rhamnolipid (■, solid line shows predicted simulation). Data from Figure 1. The x-axis shows the number of pore volumes after removal of phenanthrene had started.

of phenanthrene, observed and predicted effluent concentrations were not increased by the factor *E* as phenanthrene was depleted from the equilibrium domain before the effluent concentrations could reach their maximal value (Figure 2A,B).

A large fraction of the phenanthrene was removed within a few pore volumes. For instance, the number of pore volumes needed to achieve 50% removal was reduced by a factor of 2–5 by the addition of rhamnolipid (Figure 3, Table 3). This reduction was close to the ratio of the retardation factors for phenanthrene in the absence and in the presence of rhamnolipid (*R/R'*), as is expected when the agent is uniformly present in the column during the entire desorption phase and provided that the contaminant is not depleted from the instantaneous sorption domain before this percentage of removal is reached. When *K_d* is high, *R/R'* will approach the enhancement factor *E*. This implies that the effect of rhamnolipid on the removal of 50% of the phenanthrene was essentially determined by *E*, and therefore by *K_c* and *C_{HOC,0}*.

Cyclodextrin-enhanced transport of several HOCs through two different soils was also predicted well by the *K_c* (4). The micelle partitioning constant of phenanthrene into rhamnolipid micelles is similar to values reported for phenanthrene and several synthetic surfactants, including Triton X-100 (19, 41). However, corrected for the differences in concentration of surfactant used, rhamnolipid was more efficient in enhancing phenanthrene removal than Triton X-100 (9). Rhamnolipid also was more efficient (on a g/L base) in enhancing phenanthrene removal than cyclodextrin (4, 42), because of the higher *K_c* value, and as efficient as dissolved organic matter (3).

The initial period of fast phenanthrene removal was followed by an extended period where phenanthrene was

eluted at low concentrations, as was the case in the absence of rhamnolipid. The number of pore volumes needed to achieve 90% removal was reduced up to a factor of 3.5 as compared to treatment without rhamnolipid (Figure 3, Table 3). This reduction was smaller than *R/R'* and generally also smaller than the reduction in 50% removal times. Ultimately, phenanthrene removal was determined by the rate of desorption, as characterized by *F* and *k₋₁*. Therefore, the reduction by rhamnolipid of the time required to reach a certain percentage removal was predicted by the two-component advective-dispersive model (eqs 6–11) to decrease from *E* for low removal percentages to unity for complete removal (Figure 3). The enhanced removal profiles of benzo[a]pyrene by dissolved organic matter from aquifer sediment (2) and of phenanthrene by Triton X-100 from a sandy soil (9) also showed extended tailing that followed the initial fast removal. Apparently, solubilizing agents generally cannot completely overcome the kinetic constraints that cause desorption of contaminants to be rate limited.

Effect of Rhamnolipid on Removal of Phenanthrene from Rate-Limited Domains. To investigate rhamnolipid-enhanced removal of phenanthrene from soil in more detail, two sets of experiments were performed. In the first set of experiments, transport of phenanthrene through Eustis and Borden soils was measured in a background solution of rhamnolipid (Figure 4, Table 2). The mobility of phenanthrene in the presence of 500 mg/L rhamnolipid was enhanced as compared to the situation where no rhamnolipid was present, as was predicted on the basis of eq 9. The extent of tailing in the breakthrough curve of phenanthrene was greatly reduced for both soils, which could not be explained by effects of rhamnolipid on sorptive partitioning of phenanthrene only (see predicted simulation with *k₋₁'* = *k₋₁*, Figure 4). This indicates that rhamnolipid increased the desorption rate constants, although desorption of phenanthrene in the presence of rhamnolipid still was rate limited (compare with simulation using *k₋₁'* → ∞, Figure 4). This trend was the same for the Borden material. At a concentration of 20 mg/L, rhamnolipid did not affect phenanthrene transport through Eustis soil as *R'* was not significantly different from *R* (Table 2) and the breakthrough curve was well predicted using *k₋₁*.

In the second set of experiments, Eustis soil was contaminated with phenanthrene, and 88% of the phenanthrene present in the column was removed by elution with electrolyte solution. Subsequently, elution was continued with a solution containing 500 mg/L rhamnolipid. This resulted in a temporary increase of the effluent phenanthrene concentration (Figure 5). Because the aqueous phenanthrene concentration was low at the time of introduction of rhamnolipid (*C_{effluent}*/*C_{HOC,0}* = 0.09), the concentration gradient of phenanthrene between the aqueous phase and rate-limited sorption domain could only be increased to a small extent. An influence of rhamnolipid on the desorption kinetics of phenanthrene will be especially observable in this situation. In 50 pore volumes following the addition of

TABLE 3. Effect of Rhamnolipid on Phenanthrene Removal

	50% removal			90% removal			$(R/R')_{\text{predicted}}^a$
	without rhamnolipid ^b	with rhamnolipid ^{b,c}	reduction ratio ^d	without rhamnolipid ^b	with rhamnolipid ^{b,c}	reduction ratio ^d	
Eustis	88	17	5.3	337	135	2.5	5.4
Borden	5.3	3.1	1.7	22	9.6	2.3	3.0
Vinton	9.8	3.6	2.7	53	51	1.0	3.8
Bonify	91	19	4.8	585	166	3.5	5.5

^a Calculated from eqs 12 and 9 using parameter values obtained from breakthrough curves of phenanthrene in the absence of rhamnolipid (Table 2). ^b Data represent the number of pore volumes required to obtain 50% and 90% removal of total mass of phenanthrene present in the column. ^c The rhamnolipid concentration was 500 mg/L. ^d Ratio of the number of pore volumes required to achieve the removal percentage given when eluting without rhamnolipid and the number of pore volumes required when eluting with rhamnolipid.

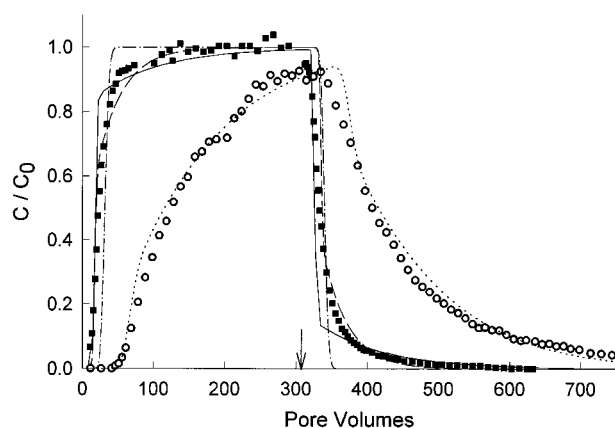


FIGURE 4. Transport of phenanthrene through Eustis soil in the absence of rhamnolipid (○, replotted from Figure 1, dotted line shows best fit) or in the presence of 500 mg/L rhamnolipid (■). From the time indicated by the arrow, elution was continued with a phenanthrene-free solution. Lines show predicted simulations with $k_{-1}' = k_{-1}$ (solid line); $k_{-1}' = 3k_{-1}$ (dashed line); or $k_{-1}' \rightarrow \infty$ (dash-dotted line).

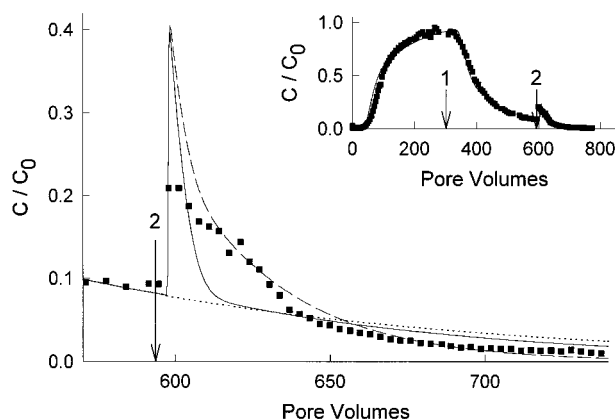


FIGURE 5. Effect of rhamnolipid on the removal of phenanthrene from rate-limited domains in Eustis soil. A column was eluted with a solution containing phenanthrene ($C_{\text{phen},0}$). From the time indicated by the first arrow (inset), the column was eluted with a solution without rhamnolipid and phenanthrene and from the time indicated by the second arrow (main graph, inset) with a solution containing 500 mg/L rhamnolipid. Experimental phenanthrene data (○). Lines show predicted simulations with $k_{-1}' = k_{-1}$ (solid line); $k_{-1}' = 3k_{-1}$ (dashed line); or when no rhamnolipid would have been applied (dotted line).

rhamnolipid, 1.3 times more phenanthrene was removed during elution with rhamnolipid than was predicted based on the assumption that rhamnolipid does not influence the first-order desorption rate constant of phenanthrene (Figure 5, data and solid line, respectively). Conversely, 1.5 times

more phenanthrene was predicted to be removed for a simulation conducted using a first-order desorption rate constant that increased 3-fold in the presence of rhamnolipid (Figure 5, dashed line).

In both sets of experiments, comparison of the experimental data with predictions showed that rhamnolipid enhanced the (de)sorption rates of phenanthrene to a greater extent than was expected based on micellar partitioning only. In terms of the two-domain conceptualization, this implies that rhamnolipid, in addition to influencing sorption equilibria, increased the first-order desorption rate coefficient of phenanthrene. A direct effect of surfactants on desorption rate coefficients of organic compounds has been reported previously (43–45). Deitsch and Smith (43) and Yeom et al. (44) hypothesized that the influence of surfactant on the desorption kinetics of HOC was related to surfactant-induced swelling of the sorbent, which would increase the matrix diffusivity of the sorbate. The same hypothesis has been used to explain the effect of cosolvents on first-order desorption rate coefficients of HOC (7). Interaction between surfactant and soil is required for surfactant to influence the desorption kinetics of HOC. Given that in our system rhamnolipid adsorption to soil was weak and, more important, not strictly correlated with the soil organic carbon content, it is not surprising that the increase in desorption rate coefficients observed herein was smaller than observed previously for more strongly sorbed surfactants (44).

Summarizing, we have found that rhamnolipid can be used to enhance the removal of a major portion of sorbed phenanthrene from soil relative to treatment without rhamnolipid. The enhanced removal of phenanthrene by rhamnolipid is largely due to partitioning of phenanthrene into micelles. Total removal of phenanthrene is ultimately determined by the desorption rate of the contaminant, which is significantly increased in the presence of rhamnolipid. This is of importance for the use of rhamnolipid for soil remediation and the ability of rhamnolipid to increase the bioavailability of sorbed substrate.

Acknowledgments

This research was funded by the Dutch IOP Environmental Biotechnology Program (Contract IOP91224). W.H.N. acknowledges the Dutch Organization for Scientific Research (NWO) for a traveling grant to Tucson (Grant SIR 14-1548) and Joseph J. Piatt and Qinhong Hu for their assistance.

Literature Cited

- Enfield, C. G.; Bengtsson, G.; Lindqvist, R. *Environ. Sci. Technol.* **1989**, *23*, 1278–1286.
- Johnson, W. P.; Amy, G. L. *Environ. Sci. Technol.* **1995**, *29*, 807–817.
- Magee, B. R.; Lion, L. W.; Lemley, A. T. *Environ. Sci. Technol.* **1991**, *25*, 323–331.
- Brusseau, M. L.; Wang, X.; Hu, Q. *Environ. Sci. Technol.* **1994**, *28*, 952–956.

- (5) Augustijn, D. C. M.; Jessup, R. E.; Rao, P. S. C.; Wood, A. L. *J. Environ. Eng.* **1994**, *120*, 42–57.
- (6) Imhoff, P. T.; Gleyzer, S. N.; McBride, J. F.; Vancho, L. A.; Okuda, I.; Miller, C. T. *Environ. Sci. Technol.* **1995**, *29*, 1966–1976.
- (7) Brusseau, M. L.; Wood, A. L.; Rao, P. S. C. *Environ. Sci. Technol.* **1991**, *25*, 903–910.
- (8) Abdul, A. S.; Gibson, T. L.; Rai, D. N. *Ground Water* **1990**, *28*, 920–926.
- (9) Adeel, Z.; Luthy, R. G.; Edwards, D. A. *Water Resour. Res.* **1995**, *31*, 2035–2045.
- (10) Okuda, I.; McBride, J. F.; Gleyzer, S. N.; Miller, C. T. *Environ. Sci. Technol.* **1996**, *30*, 1852–1860.
- (11) Pennell, K. D.; Abriola, L. M.; Weber, W. J. *Environ. Sci. Technol.* **1993**, *27*, 2332–2340.
- (12) Wilson, D. J.; Clark, A. N. *Sep. Sci. Technol.* **1991**, *26*, 1177–1194.
- (13) Zhang, Y.; Miller, R. M. *Appl. Environ. Microbiol.* **1992**, *58*, 3276–3282.
- (14) Hunt, W. P.; Robinson, K. G.; Gosh, M. M. In *Hydrocarbon Bioremediation*; Hinchee, R. E., Alleman, B. C., Hoeppe, R. E., Miller, R. N., Eds.; Lewis Publishers: Boca Raton, 1994; p 318.
- (15) Hisatsuka, K.; Nakahara, T.; Sano, N.; Yamada, K. *Agric. Biol. Chem.* **1971**, *35*, 686–692.
- (16) Van-Dyke, M. I.; Couture, P.; Brauer, M.; Lee, H.; Trevors, J. T. *Can. J. Microbiol.* **1993**, *39*, 1071–1078.
- (17) Herman, D. C.; Artiola, J. F.; Miller, R. M. *Environ. Sci. Technol.* **1995**, *29*, 2280–2285.
- (18) Brusseau, M. L.; Jessup, R. E.; Rao, P. S. C. *Environ. Sci. Technol.* **1990**, *24*, 727–735.
- (19) Edwards, D. A.; Luthy, R. G.; Liu, Z. *Environ. Sci. Technol.* **1991**, *25*, 127–133.
- (20) Almgren, M.; Grieser, F.; Thomas, J. K. *J. Am. Chem. Soc.* **1979**, *101*, 279–291.
- (21) Kowalczyk, A. A.; Večér, J.; Hodgeson, B. W.; Keene, J. P.; Dale, R. E. *Langmuir* **1996**, *12*, 4358–4371.
- (22) Smith, J. A.; Sahoo, D.; McLellan, H. M.; Imbrigiotta, T. E. *Environ. Sci. Technol.* **1997**, *31*, 3565–3572.
- (23) Brusseau, M. L.; Rao, P. S. C.; Jessup, R. E.; Davidson, J. M. *J. Contam. Hydrol.* **1989**, *4*, 223–240.
- (24) Sheng, G.; Xu, S.; Boyd, S. A. *Environ. Sci. Technol.* **1996**, *30*, 1553–1557.
- (25) Sun, S.; Inskeep, W. P.; Boyd, S. A. *Environ. Sci. Technol.* **1995**, *29*, 903–913.
- (26) Edwards, D. A.; Adeel, Z.; Luthy, R. G. *Environ. Sci. Technol.* **1994**, *28*, 1550–1560.
- (27) Monticone, V.; Mannebach, M. H.; Treiner, C. *Langmuir* **1994**, *10*, 2395–2398.
- (28) Park, J.-W.; Jaffé, P. R. *Environ. Sci. Technol.* **1993**, *27*, 2559–2656.
- (29) Valsaraj, K. T. *Sep. Sci. Technol.* **1989**, *24*, 1191–1206.
- (30) Brusseau, M. L. *Water Resour. Res.* **1993**, *29*, 1071–1080.
- (31) Kwok, W.; Hayes, R. E.; Nasr-el-din, H. A. *Can. J. Chem. Eng.* **1995**, *73*, 705–716.
- (32) Ishigami, Y.; Gama, Y.; Nagahora, H.; Yamaguchi, M.; Nakahara, H.; Kamata, T. *Chem. Lett.* **1987**, 763–766.
- (33) Champion, J. T.; Gilkey, J. C.; Lamparski, H.; Retterer, J.; Miller, R. M. *J. Colloid Interface Sci.* **1995**, *170*, 569–574.
- (34) Chandrasekaran, E. V.; BeMiller, J. N. In *Methods in Carbohydrate Chemistry*; Whistler, R. L., BeMiller, J. N., Eds.; Academic Press: New York, 1980; Vol. 8, pp 89–96.
- (35) May, W. E.; Waslik, S. P.; Freeman, D. M. *Anal. Chem.* **1978**, *50*, 175–179.
- (36) Ball, W. P.; Roberts, P. V. *Environ. Sci. Technol.* **1991**, *25*, 1223–1237.
- (37) Parker, J. C.; Van Genuchten, M. Th. Determining transport parameters from laboratory and field tracer experiments. Bulletin 84-3, Virginia Agricultural Experiment Station: Blacksburg, 1984.
- (38) Valocchi, A. J. *Water Resour. Res.* **1985**, *21*, 808–820.
- (39) Zhang, Y.; Maier, W. J.; Miller, R. M. *Environ. Sci. Technol.* **1997**, *31*, 2211–2217.
- (40) Brusseau, M. L.; Jessup, R. E.; Rao, P. S. C. *Environ. Sci. Technol.* **1991**, *25*, 134–142.
- (41) Tiehm, A. *Appl. Environ. Microbiol.* **1994**, *60*, 258–263.
- (42) Brusseau, M. L.; Wang, X.; Wang, W.-Z. *Environ. Sci. Technol.* **1997**, *31*, 1087–1092.
- (43) Deitsch, J. J.; Smith, J. A. *Environ. Sci. Technol.* **1995**, *29*, 1069–1080.
- (44) Yeom, I. T.; Ghosh, M. M.; Cox, C. D. *Environ. Sci. Technol.* **1996**, *30*, 1589–1595.
- (45) Sahoo, D.; Smith, J. A. *Environ. Sci. Technol.* **1997**, *31*, 1910–1915.
- (46) Rao, P. S. C.; Davidson, J. M.; Jessup, R. E.; Selim, H. M. *Soil Sci. Soc. Am. J.* **1979**, *43*, 22–28.
- (47) Young, M. H.; Wierenga, P. J.; Mancino, C. F. *Soil Sci.* **1996**, *161*, 491–501.

Received for review August 19, 1997. Revised manuscript received March 12, 1998. Accepted March 20, 1998.

ES970739H